XLI CILAMCE
XLI Ibero-Latin American Congress on Computational Methods in Engineering
16-19 November, 2020 FOZ DO IGUAÇU PARANÁ - BRAZIL

PRELIMINARY RESULTS ON 3D CONTACT SHAPE OPTIMIZATION WITH THE BOUNDARY ELEMENT METHOD

Cristiano J. B. Ubessi[1], Filipe P. Geiger[2], Rogério J. Marczak[3]

[1,3]*Departamento de Engenharia Mecânica, Universidade Federal do Rio Grande do Sul, Brazil*
Rua Sarmento Leite 425, 90050-170, RS, Brasil
[1]*cristiano.ubessi@ufrgs.br,*[3]*rato@mecanica.ufrgs.br*
[2]*Programa de Pós Graduação em Engenharia Mecânica, Universidade Federal do Rio Grande do Sul, Brazil*
Rua Sarmento Leite 425, 90050-170, RS, Brasil
filipe.geiger@ufrgs.br

Abstract. This work presents preliminary results applying the Boundary Element Method (BEM) as a structural sensitivity kernel under a contact shape optimization procedure for 3D problems involving anisotropic materials under contact, using the Complex-Step Method (CSM) to obtain sensitivities of objective function and restrictions to the variation of design parameters. In this preliminary work, we present the results for the isotropic case. An important aspect regarding the fatigue life of ductile materials subject to contact conditions is the occurrence of the maximum shear stress below the surface. The examples analyzed with the present methodology explore the optimization of shape aiming towards a smooth stress distribution along the blade root surface. The optimization procedure follows the SLP paradigm. This BEM based methodology can avoid the need for extreme mesh refinements reducing computational cost while obtaining useable results.

Keywords: Contact shape optimization, Complex-Step Method, Anisotropic BEM

1 Introduction

A common characteristic of metallic surfaces in contact is due to the relatively high stiffness of these materials when compared with the level of acceptable strains, such that, small changes in the initial separation between these surfaces can result in extremely different contact pressure distribution. As these are key variables in the fatigue life of these components, optimization of the contact shape as well as the initial separation should be mandatory for nearly all components under oscillating loads. Another aspect of components under cyclic contact loading is that fatigue can occur at a small scale just below the region of slip, a mechanism which is commonly known as fretting fatigue Szolwinski and Farris [1].

Over the last few decades, the shape and topology optimization of problems involving contact is a recurrent theme in the literature. Since the pioneer works of Haslinger et al. [2], which has proven the total potential energy when used as a cost function can lead to a constant distribution of flux on the contact surface, and the works of Haslinger [3] and Klarbring and Haslinger [4] where the same principles were applied to obtain a constant distribution of contact pressure. Fancello et al. [5] compared the two cost functions from [2] and [6] with considerable differences in the pressure distribution of the optimal shape. Haslinger [7] demonstrated that the functional on contact shape optimization is only directionally differentiable, and their derivatives result in another quadratic programming problem. Hilding et al. [8] employed a p-norm approach for contact distributions modifying the structure shape outside of the contact region. Vondrák et al. [9] performed contact shape optimization for 3D problems using a domain decomposition method designed for parallel implementation. In the last few years, a large number of works are found dealing with topology optimization in contact problems such as Zhang and Niu [10], Niu et al. [11], and Ma et al. [12].

Although one can consider a variety of objective functions, Calvo and Gracia [13] showed that the vast majority of them result in a boundary-only integral formulation in which the BEM has a clear advantage. As pointed by Fancello [14], a known disadvantage of the FEM in the context of optimization algorithms is poor accuracy on boundary results. The BEM is not only well-known for its accuracy in the solution of contact problems but also has been successfully applied to obtain shape sensitivities. In Sfantos and Aliabadi [15], Tafreshi [16]

Tafreshi [17] the direct or implicit differentiation of the integral equations is carried out for 2D problems. In Erman and Fenner [18] the author performs analytic differentiation of the boundary integral equations. In Mundstock and Marczak [22] the CS method has also been used in a shape sensitivity framework for plane elasticity. In previous work (Ubessi and Marczak [23]) we have devised an implementation of this method in contact problems with the BEM, which will be used in this work as the core of the optimization procedures.

The key points in using the CS-BEM approach for obtaining shape sensitivity in contact problems are: (i) The CS method is exact and therefore does not even compare to FD, and has a straightforward implementation, does not necessarily imply modifications in the existing code if complex algebra is enabled; (ii) The CS avoids the increased singularity involved in analytic sensitivity. (iii) In the context of numerical methods, BEM precision on tractions leads to a better approximation of shape derivatives, especially in contact problems.

This paper presents initial results in 3D contact optimization using an efficient methodology to evaluate shape sensitivities with the BEM as the structural analysis framework and is organized as follows: Section 2 presents the formulation of the contact shape optimization problem. Section 3 briefly describes the methodology for BEM contact shape sensitivity. Section 4 shows the initial structural optimization problem setting and the results obtained for this preliminary example. We close this work in Section 5 drawing the main conclusions from this analysis and raise some questions on potential aspects to be further studied in future work.

2 Contact shape optimization problem statement

The optimal shape for the contacting surface, aiming for a constant distribution of contact pressure, can be thought of as the minimization of the maximum contact pressure. Although an obvious choice, this function is not well-behaved, and may rapidly become unstable, as the maximum pressure changes from one node to another. According to Hilding et al. [8], in problems with singularities, which are generally the ones one would be interested in performing the optimization, this function is not well-defined and of course non-differentiable. A more commonly used and accepted measure for the smoothness of the contact pressure distribution is the L_2-norm of the contact pressure, i.e.,

$$\|p\|_{L^2(\Gamma_c)} = \left(\int_{\Gamma_c} p^2 d\Gamma \right)^{1/2}, \tag{1}$$

where p is the contact pressure and Γ_c is the contact surface. As noted by Hilding et al. [8], this function is only Lipschitz continuous, at the limit it has at least a directional derivative. As long as the total contact force does not increase, it is clear that this function is minimized if the contact pressure is constant over Γ_c. Any variation from the constant distribution will cause this integral to rapidly increase, providing some form of convexity for the problem.

Let $\mathbf{x}$ be the vector containing all design variables x_i, the optimization problem statement is

$$\begin{aligned} \underset{\mathbf{x}}{\text{Min}} \quad & \|p\|_{L^2(\Gamma_c)} \\ \text{subject to} \quad & V(\mathbf{x}) \leq V(\mathbf{x}_0) \\ & x_{\text{min}} \leq x \leq x_{\text{max}} \end{aligned} \tag{2}$$

where we have considered a maximum volume restriction, as well as maximum (x_{min}) and minimum (x_{max}) bounds for any of the design variables $\mathbf{x}$. The optimization procedure adopted in this work is based in the sequential linear programming (SLP) algorithm from [24], in which the non-linear objective function and restrictions are approximated by a sequence of linearized functions, using a Taylor series expansion. For each iteration the following linear programming problem has to be solved:

$$\begin{aligned} \underset{\mathbf{x}}{\text{Min}} \quad & f(\mathbf{x}_0) + \sum_{i=1}^{n} (x_i - x_{0i}) \left(\frac{\partial f}{\partial x_i} \right) \Big|_{x_o} \\ \text{subject to} \quad & (\mathbf{x}_0) + \sum_{i=1}^{n} (x_i - x_{0i}) \left(\frac{\partial g_j}{\partial x_i} \right) \Big|_{x_o} \geq 0 \\ & x_i \geq \max(x_{min}, x_{0i} - a_{li}) \\ & x_i \leq \min(x_{max}, x_{0i} + a_{ui}) \end{aligned} \tag{3}$$

where x_{0i} is the initial value of the design variable at the SLP iteration.

$\left(\frac{\partial f}{\partial x_i} \right) \big|_{x_o}$ and $\left(\frac{\partial g_j}{\partial x_i} \right) \big|_{x_o}$ are the sensitivities of $f(x)$, and of $g_j(x)$, evaluated at the coordinate point x_0. The last two sets of constraints on the design variables, incorporate the move limits a_{li} and a_{ui} being the lower and

upper bounds on the allowed change in x_i in each iteration respectively, as well as the lower and upper bounds for the design variables along the entire problem x_{min} and x_{max}.

This SLP scheme was chosen deliberately due to its simplicity. Therefore, other methods such as the method of moving asymptotes used by Hilding et al. [8] or the interior point method found in [5] are expected to deliver even better performance. The solution of the linear programming problem is directly applied to the next iteration. We have not used a solution scaling scheme between iterations to update the objective function, as it would need to recalculate the whole problem several times. A relatively small move limit was found to help the next solution do not fall too far from the optimal point.

3 Shape sensitivity from complex-stepped boundary integral equations

The CS method is entirely based on the Cauchy-Riemann equations, observed initially by Lyness and Moler [25], and the properties of analytical functions, which was later shown in the form it is actually used by Squire and Trapp [26], formulated using a Taylor series expansion of $f(x + \mathrm{i}\Delta x)$, which, isolating completely the first derivative $f'(x)$ to the left-hand side, one gets

$$f'(x) = \frac{\mathrm{Im}\left[f(x + \mathrm{i}\Delta x)\right]}{\Delta x} + \mathcal{O}(\Delta x^2). \tag{4}$$

As the truncated terms of the series are lower than Δx^2, it yields quadratic convergence. The CS does not imply a differentiation, so it does not have cancellation error such as FD, and the increment Δx can be lower in magnitude than machine precision, i.e., ($\varepsilon^D = 2^{-52} \approx 10^{-16}$), and the truncation error $\mathcal{O}(\Delta x^2)$ vanishes by round off, making the method exact up to rounding error, and insensitive to the step size.

To formulate the CS-BEM in a similar fashion as the conventional BEM, let us consider a design variable γ, and let us add an increment $\Delta\gamma$ to its imaginary part, such that $\hat{\gamma} = \gamma + \mathrm{i}\Delta\gamma$. One can then write the boundary integral equation considering either source $\mathbf{x}$ and field $\mathbf{y}$ points complex, i.e.,

$$\mathbf{C}\mathbf{u} + \fint_\Gamma \mathbf{T}(\mathbf{x} + \mathrm{i}\Delta\mathbf{x})\,\mathbf{u}\,\mathrm{d}\Gamma = \int_\Gamma \mathbf{U}(\mathbf{x} + \mathrm{i}\Delta\mathbf{x})\,\mathbf{t}\,\mathrm{d}\Gamma + \int_\Omega \mathbf{U}(\mathbf{x} + \mathrm{i}\Delta\mathbf{x})\,\mathbf{b}\,\mathrm{d}\Omega, \tag{5}$$

where $f(\mathbf{x} + \mathrm{i}\Delta\mathbf{x})$ denotes that source and field are complex. Notice that eq. (5) and the conventional real-valued BEM equations are virtually the same. The usual fundamental solutions ($\mathbf{T}$ and $\mathbf{U}$) are the ones proposed recently in [27]. $\fint(\cdot)\mathrm{d}\Gamma$ denotes the Cauchy Principal Value of integral $\int(\cdot)\mathrm{d}\Gamma$.

After the element discretization of boundary Γ and a collocation process for all source points results in the standard BEM set of linear equations,

$$\mathbf{H}(\mathbf{x} + \mathrm{i}\Delta\mathbf{x})\mathbf{u} = \mathbf{G}(\mathbf{x} + \mathrm{i}\Delta\mathbf{x})\mathbf{p}, \tag{6}$$

which can be solved for the unknowns on Γ. The solution vector $\mathbf{z}$ real part corresponds to displacement and traction unknowns,

$$\mathbf{u} = \mathrm{Re}[\mathbf{z}^{\mathbf{u}}], \quad \text{and,} \quad \mathbf{p} = \mathrm{Re}[\mathbf{z}^{\mathbf{p}}], \tag{7}$$

and their sensitivities with respect to the design variable γ are

$$\frac{\partial \mathbf{u}}{\partial \gamma} = \frac{\mathrm{Im}\left[\mathbf{z}^{\mathbf{u}}\right]}{\Delta\gamma}, \quad \frac{\partial \mathbf{p}}{\partial \gamma} = \frac{\mathrm{Im}\left[\mathbf{z}^{\mathbf{p}}\right]}{\Delta\gamma}. \tag{8}$$

Notice that the above passages are exactly the same for CSBEM and the conventional BEM, only differing on the complex variables. For details on the BEM contact implementation, one should refer to Ubessi and Marczak [23].

3.1 Shape derivatives of objective and constraint functions

After updating the parts of the system of linear equations affected by the complex step in design variable $\mathbf{x}_i$, and solving for the complex solution vector $\hat{\mathbf{z}}$, the sensitivity of the objective function eq. (1) to variable x_i is evaluated by:

$$\frac{d\left\|p\right\|_{L^2(\Gamma_c)}}{d\gamma_i} = \frac{\mathrm{Im}\left[\sum_{j=1}^{nc}\left(\int_{\Gamma_c^j} p(\mathbf{x} + i\Delta\mathbf{x})^2 d\Gamma\right)^{1/2}\right]}{\Delta\mathbf{x}}, \tag{9}$$

The volume is calculated using a boundary only integral by Brebbia et al. [31], and its sensitivity is evaluated in the same fashion, right after the new volume was evaluated for the new design variable vector $\mathbf{x}$

$$\frac{dV}{d\gamma_i} = \frac{\text{Im}\left[\hat{V}(\mathbf{x} + \mathrm{i}\Delta\mathbf{x})\right]}{\Delta\mathbf{x}}, \tag{10}$$

where $\hat{V}$ is the complex volume resulting when variable $\mathbf{x}_i$ receive an increment $\Delta\mathbf{x}$ at its imaginary part.

4 Preliminary results on shape optimization

The geometry of the example analyzed in this work is due to Papanikos et al. [32], a 30° section cut from a 12 blade rotor. This problem provides a common application in which the contact geometry and material orientation may be optimized to increase fatigue and fretting life. The thickness for both rotor and blade was set to 10mm. At the section cut, a displacement restriction in the element normal direction has been applied to ensure rotational symmetry, and the y displacement for the rotor and blade was constrained, meaning symmetry along the axial direction. To simplify the analysis and avoid domain integration a point force was applied at the blade center of mass consistent to an angular speed of 1000rpm. The coefficient of friction for the contact formulation was considered as $\mu = 0.25$. The material density for the blade and rotor is $\rho = 4429\text{kg}/\text{m}^3$, and the elastic constants are $E = 114$ GPa and $\nu = 0.33$.

The BEM discontinuity for definition of coloccation points was also set to the same value, $\eta = 0.75$, and Fig. 1a shows the mesh considered for thus problem.

To simplify this initial example, we considered the shape to be continuous along the Z-axis. The nodes were allowed to move in the normal direction to the initial contact surface, at the flank angle of 20°. The design variables in the optimization problem are the position of these groups of nodes, relative to their initial position, as shown in Fig. 1b. This case resulted in five design variables.

Regarding the SLP problem, the upper and lower bounds on the initial move limits were set to $x_{li} = x_{ui} = 5e - 3$. The maximum allowed position for the nodes was set to zero, i.e., only material removal was allowed $x_i^{\max} = 0$, while the lower limit for this movement, was set to $x_i^{\min} = -1 \times 10^{-2}$.

In Fig. 2a we present the objective function and move limits, normalized with their initial values as the SLP algorithm iterations progress. Also, to investigate any noticeable variation in the maximum displacement for the blade due to the different contact forces, we show the difference between the maximum initial displacement at the blade tip and the current iteration ones. As the variation is rather small, we show this variation in percent. In the final geometry, the volume variation was -1×10^{-5} of the initial volume.

Due to mass distribution, the contact pressures are not constant through the depth of the blade, being higher at the line of nodes near the symmetry plane, therefore the 3D treatment is still useful in this case. The initial pressure distribution for this problem at this position is shown in Fig. 2b, as well as the one obtained after 15 iterations of the SLP process.

5 Conclusion

The CS method, even in this simple direct increment of the design variables, resulted in very reliable and consistent derivatives for the contact problem. Even with this simple SLP approach very good results were obtained, with a few tests to find a good value for the move limits. Also, the choice of adjusting one side only, which can be seen as adjusting the initial separation between the two bodies, limits the possibility of shape modification. Changing the two bodies' shape at the same time maybe also of interest, for example, to find a joint geometry with no initial separation and desirable pressure distribution.

In this work, we found that by updating the BEM matrices only for the complex parts, resulted in a fast algorithm, without compromising the original generality of the assembly routines. In the adopted scheme where several mesh nodes were incremented, a considerable number of collocation points were affected by the complex-step. As noted by Haveroth et al. [20], even the analytical methods also have to solve the system of linear equations for a few different right-hand side vectors. In future work, we aim to also test if a complex-analytical scheme as is proposed by the authors, is applicable in contact problems.

The main advantage of using the BEM in this optimization example is that even using a very coarse mesh and linear elements we obtained good estimates of an enhanced contact shape for obtaining pressure distributions according to our needs. Another possibility for future investigations is to determine if a coarser mesh can be used to calculate shape sensitivities and a finer one used between iterations where the objective function is updated and verified, as ideally, the geometry is driven by some spline parameters which smooth out the mesh changes. Spline defined surfaces also may be able to reduce the total design variables and therefore the number of sensitivity evaluations needed in each iteration, while using a finer mesh.

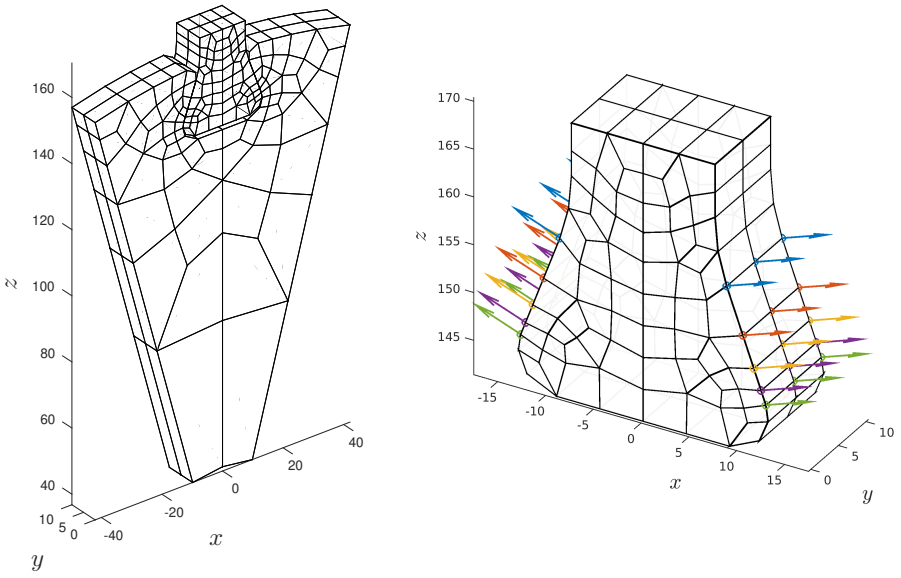

(a) (b)

Figure 1. (a) Simplified linear element mesh for the optimization problem. (b) Sets of design nodes and shape sensitivity evaluation direction.

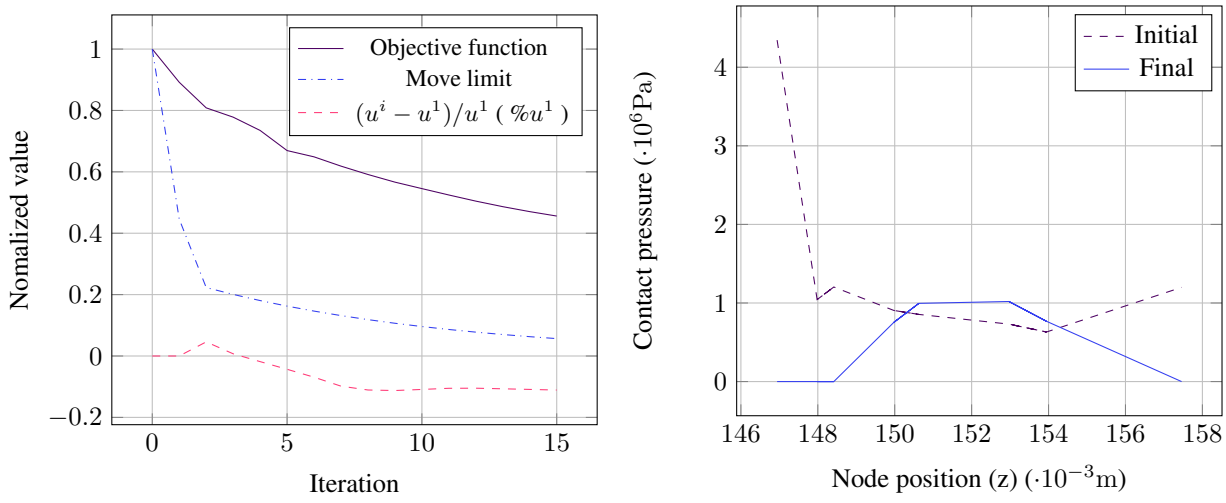

(a) (b)

Figure 2. (a) Normalized objective function and move limit along the SLP iterations, and percentage variation of maximum blade displacement relative to initial. (b) Initial and final contact pressures near the symmetry plane of the blade, at $y = 10$.

Acknowledgements. C. Ubessi, F. Geiger, and R. Marczak are grateful to the Brazilian CAPES and CNPq for financial support.

Authorship statement. The authors hereby confirm that they are the sole liable persons responsible for the authorship of this work, and that all material that has been herein included as part of the present paper is either the property (and authorship) of the authors, or has the permission of the owners to be included here.

References

[1] Szolwinski, M. P. & Farris, T. N., 1996. Mechanics of fretting fatigue crack formation. *Wear*, vol. 198, n. 1, pp. 93 – 107.

[2] Haslinger, J., Neittaanmäki, P., Tiihonen, T., & Kaarna, A., 1988. Optimal shape design and unilateral boundary value problems: Part ii. *OPTIMAL CONTROL APPLICATIONS & METHODS*, vol. 9, pp. 145–163.
[3] Haslinger, J., 1991. Shape optimization in unilateral boundary value problems. In *Unilateral Problems in Structural Analysis IV*, pp. 51–55. Springer.
[4] Klarbring, A. & Haslinger, J., 1993. On almost constant contact stress distributions by shape optimization. *Structural Optimization*, vol. 5, pp. 213–216.
[5] Fancello, E., Haslinger, J., & Feijoo, R., 1995. Numerical comparison between two cost functions in contact shape optimization. *Structural Optimization*, vol. 9, n. 1, pp. 57–68.
[6] Haslinger, J. & Klarbring, A., 1993. Shape optimization in unilateral contact problems using generalized reciprocal energy as objective functional. *Nonlinear Analysis: Theory, Methods & Applications*, vol. 21, n. 11, pp. 815–834.
[7] Haslinger, J., 1999. Contact shape optimization based on the reciprocal variational formulation. *Applications of Mathematics*, vol. 44, n. 5, pp. 321–358.
[8] Hilding, D., Torstenfelt, B., & Klarbring, A., 2001. A computational methodology for shape optimization of structures in frictionless contact. *Computer methods in applied mechanics and engineering*, vol. 190, n. 31, pp. 4043–4060.
[9] Vondrák, V., Kozubek, T., Markopoulos, A., & Dostál, Z., 2010. Parallel solution of contact shape optimization problems based on total feti domain decomposition method. *Structural and Multidisciplinary Optimization*, vol. 42, n. 6, pp. 955–964.
[10] Zhang, W. & Niu, C., 2018. A linear relaxation model for shape optimization of constrained contact force problem. *Computers & Structures*, vol. 200, pp. 53 – 67.
[11] Niu, C., Zhang, W., & Gao, T., 2019. Topology optimization of continuum structures for the uniformity of contact pressures. *Struct. Multidiscip. Optim.*, vol. 60, n. 1, pp. 185–210.
[12] Ma, Y., Chen, X., & Zuo, W., 2020. Equivalent static displacements method for contact force optimization. *Structural and Multidisciplinary Optimization*, vol. 62, pp. 323–336.
[13] Calvo, E. & Gracia, L., 2001. Shape design sensitivity analysis in elasticity using the boundary element method. *Engineering Analysis with Boundary Elements*, vol. 25, n. 10, pp. 887–896. cited By 3.
[14] Fancello, E. A., 2006. Topology optimization for minimum mass design considering local failure constraints and contact boundary conditions. *Structural and Multidisciplinary Optimization*, vol. 32, pp. 229–240.
[15] Sfantos, G. & Aliabadi, M., 2006. A boundary element sensitivity formulation for contact problems using the implicit differentiation method. *Engineering Analysis with Boundary Elements*, vol. 30, n. 1, pp. 22 – 30.
[16] Tafreshi, A., 2009. Shape sensitivity analysis of composites in contact using the boundary element method. *Engineering Analysis with Boundary Elements*, vol. 33, n. 2, pp. 215 – 224.
[17] Tafreshi, A., 2011. Simulation of crack propagation in anisotropic structures using the boundary element shape sensitivities and optimisation techniques. *Engineering Analysis with Boundary Elements*, vol. 35, n. 8, pp. 984 – 995.
[18] Erman, Z. & Fenner, R. T., 1997. Three-dimensional design sensitivity analysis using a boundary integral approach. *International Journal for Numerical Methods in Engineering*, vol. 40, n. 4, pp. 637–654.
[19] Ostanin, I., Tsybulin, I., Litsarev, M., Oseledets, I., & Zorin, D., 2017. Scalable topology optimization with the kernel-independent fast multipole method. *Engineering Analysis with Boundary Elements*, vol. 83, pp. 123 – 132.
[20] Haveroth, G. A., Stahlschmidt, J., & Muñoz-Rojas, P. A., 2015. Application of the complex variable semi-analytical method for improved displacement sensitivity evaluation in geometrically nonlinear truss problems. *Latin American Journal of Solids and Structures*, vol. 12, n. 5, pp. 980–1005.
[21] Martins, J., Sturdza, P., & Alonso, J., 2001. The connection between the complex-step derivative approximation and algorithmic differentiation. In *39th Aerospace Sciences Meeting and Exhibit*, pp. 921.
[22] Mundstock, D. C. & Marczak, R. J., 2009. Boundary element sensitivity evaluation for elasticity problems using complex variable method. *Structural and Multidisciplinary Optimization*, vol. 38, n. 4, pp. 423–428.
[23] Ubessi, C. J. B. & Marczak, R. J., 2018. Sensitivity analysis of 3D frictional contact with BEM using complex-step differentiation. *Latin American Journal of Solids and Structures*, vol. 15, n. 10.
[24] Haftka, R. T. & Gürdal, Z., 2012. *Elements of structural optimization*, volume 11. Springer Science & Business Media.
[25] Lyness, J. N. & Moler, C. B., 1967. Numerical differentiation of analytic functions. *SIAM Journal on Numerical Analysis*, vol. 4, n. 2, pp. 202–210.
[26] Squire, W. & Trapp, G., 1998. Using complex variables to estimate derivatives of real functions. *SIAM Review*, vol. 40, n. 1, pp. 110–112.
[27] Buroni, F. C., Ubessi, C. J. B., Hattori, G., Saez, A., & Marczak, R. J., 2019. A fast and non-degenerate scheme for the evaluation of the 3D fundamental solution and its derivatives for fully anisotropic magneto-electro-

elastic materials. *Engineering Analysis with Boundary Elements*, vol. 105, pp. 94–103.
[28] Ubessi, C. J. B., 2019. *Non degenerate anisotropic Green's function for 3D magneto-electro-elasticity and BEM shape sensitivity framework for 3D contact in anisotropic elasticity*. Doctoral thesis, Universidade Federal do Rio Grande do Sul.
[29] Rodríguez-Tembleque, L., Buroni, F. C., Abascal, R., & Sáez, A., 2013. Analysis of FRP composites under frictional contact conditions. *International Journal of Solids and Structures*, vol. 50, n. 24, pp. 3947 – 3959.
[30] Alart, P. & Curnier, A., 1991. A mixed formulation for frictional contact problems prone to Newton like solution methods. *Computer Methods in Applied Mechanics and Engineering*, vol. 92, n. 3, pp. 353–375.
[31] Brebbia, C. A., Telles, J. C. F., & Wrobel, L. C., 2012. *Boundary element techniques: theory and applications in engineering*. Springer Science & Business Media.
[32] Papanikos, P., Meguid, S. A., & Stjepanovic, Z., 1998. Three-dimensional nonlinear finite element analysis of dovetail joints in aeroengine discs. *Finite Element Analisys and Design*, vol. 29, n. 3-4, pp. 173–186.